Adv. Polar Upper Atmos. Res., **15**, 159–177, 2001

Interhemispheric differences in the HF radar signature of the cusp region: A review through the study of a case example

Steve E. Milan and Mark Lester

Department of Physics and Astronomy, University of Leicester, Leicester LE1 7RH, U.K.

Abstract: This paper aims to provide a review of our understanding of the HF radar signatures of the cusp and transient magnetopause reconnection phenomena through the study of a case example. Two SuperDARN radars observe the conjugate cusp regions during an interval of southward IMF. These observations allow us to determine several parameters relating to the electrodynamics of the magnetopause reconnection process, including the mean reconnection voltage and the reconnection electric fields and X-line lengths in the two hemispheres. In addition, we identify several differences between the radar and flow signatures observed in the two hemispheres, specifically that flux transfer event signatures are observed in the Northern Hemisphere but not the Southern Hemisphere, and that the azimuthal component of the flow excited by reconnection is much greater in the Southern Hemisphere than in the Northern Hemisphere. We finish our discussion by identifying remaining questions regarding the interpretation of HF radar observations of the cusp.

1. Introduction

HF radars, specifically those which comprise SuperDARN (Greenwald *et al.,* 1995), have become an important tool for the study of solar wind-magnetosphere coupling processes, the radar signatures of which manifest themselves in the ionospheric cusp region. These signatures include bursts of enhanced plasma drift (Pinnock *et al.,* 1991, 1993, 1995) and poleward-moving backscatter features (Provan *et al.,* 1998, 1999; Provan and Yeoman, 1999) which have been demonstrated to be the radar equivalent of optical poleward-moving auroral forms (Milan *et al.,* 2000). These transient features are strong evidence for bursty reconnection, and indeed are found to occur in close association with magnetopause flux transfer events (FTEs) (Neudegg *et al.,* 1999, 2000), have a repetition rate similar to that of FTEs (McWilliams *et al.,* 2000), and are associated with "cusp ion steps", the low-altitude particle signature of pulsed reconnection (Lockwood *et al.,* 2001). The dayside auroral zone provides a good target for HF radars (Milan *et al.,* 1998), the equatorward edge of the backscatter appearing to correspond closely to the equatorward edge of red line aurora (Milan *et al.,* 1999b; Moen *et al.,* 2000) which has been identified as a proxy for the open/closed field line boundary (OCB). Similar conclusions were reached by Rodger *et al.* (1995); however, in their study one case example supported a correspondence between radar backscatter and red line aurora and a second found a small but significant offset between the two. We also emphasize that this auroral boundary is only a proxy for the OCB, as

Rodger and Pinnock (1997) and Rodger (2000) have argued that due to finite ion energies, field lines have convected some distance into the polar cap prior to aurora being excited in the ionosphere. However, quasi-periodic equatorward steps of this boundary, followed by poleward relaxations, have been interpreted as addenda of new open flux to the front of the polar cap by FTEs and the subsequent assimilation of this flux with the pre-existing open flux through the excitation of convective flows (Milan *et al.*, 1999b) as first suggested by Cowley and Lockwood (1992).

As yet, however, few simultaneous observations of the cusp in both Northern and Southern Hemispheres have been made (*e.g.* Pinnock *et al.*, 1991), though this should provide significant additional information pertaining to the mechanisms through which dayside coupling proceeds. For instance, it has been suggested that the dayside convection pattern could exhibit considerable asymmetries between summer and winter hemispheres as a consequence of the biases in the reconnection geometries available at the subsolar magnetopause imposed by the tilts of the dipole and rotation axes relative to the Sun-Earth line (Milan *et al.*, 2001). The purpose of the present paper is to briefly investigate similarities and differences in the HF radar signatures of the cusp region observed simultaneously in the two hemispheres, during a 90 min interval in April 1996, with the aim of reviewing our current understanding of these signatures and identifying questions that remain to be resolved regarding these signatures. We admit, however, that this review is necessarily very brief, and many aspects of dayside coupling, including a wealth of SuperDARN studies, which are not of direct relevance to the present observations have been omitted. The interested reader is directed to the review of Lu *et al.* (2001), amongst others, for further perspectives on the excitation of convection.

2. Observations

The two radars employed in this study are the Goose Bay and Halley radars of the SuperDARN chain, the two radars which comprised the original PACE system. The field-of-view of the Goose Bay radar is shown in Fig. 1, superimposed on which is the conjugate field-of-view of the Halley radar. This mapping has been achieved by determining the location of the Halley radar field-of-view in geomagnetic coordinates, reversing the sign of the latitude, effectively mapping the radar cells into the Northern Hemisphere, and transforming these new coordinates into the geographic frame of reference. We note that the term "conjugate" strictly applies only in the closed field line region, that is where a field line can be traced from its footprint in one hemisphere to a footprint in the opposite hemisphere, but we will employ it loosely in the following discussion to describe regions were symmetry considerations between the Northern and Southern Hemispheres might lead us to expect similar convection flows, even on open field lines. The conjugate radar fields-of-view overlap considerably and have very similar pointing-directions. This allows an almost direct comparison of the backscatter features observed by the two radars. For instance, at the latitude of the auroral zone beam 4 of the Goose Bay radar and the conjugate location of beam 6 of the Halley radar are separated by only 100 km in longitude, are nearly parallel, and in a magnetic coordinate system point almost meridionally. Near 1400 UT the two radar fields-of-

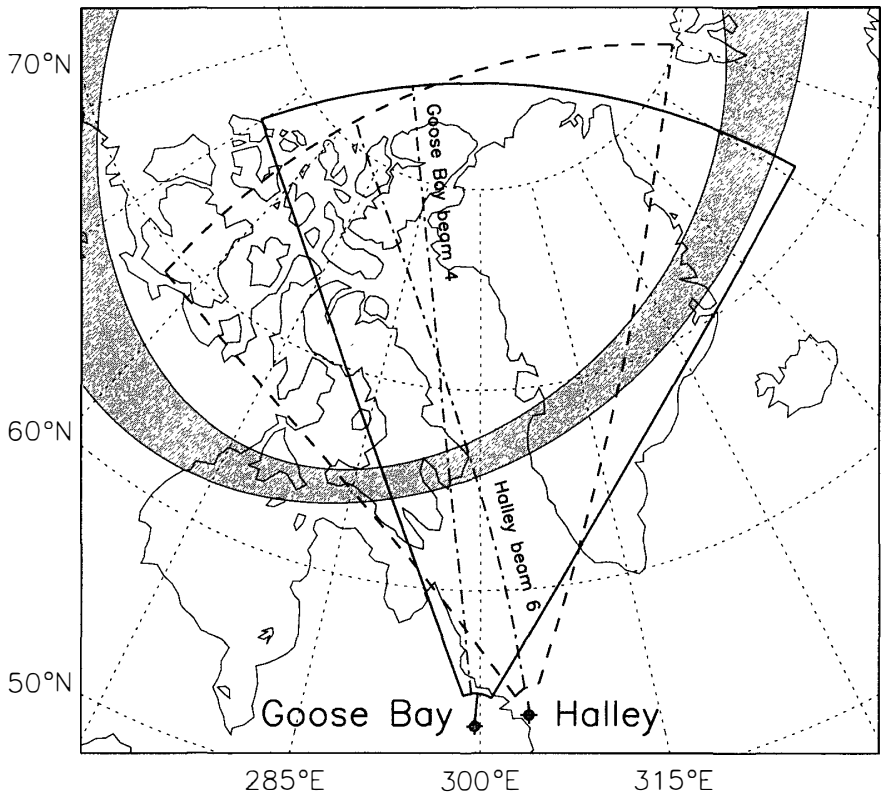

Fig. 1. A map of the Northern Hemisphere showing the location of the Goose Bay radar field-of-view (solid outline). Superimposed on this is the conjugate location of the Halley radar field-of-view (dashed outline). Beams 4 and 6 of the Goose Bay and Halley radars, respectively, are shown by dot-dashed lines. Also indicated is the location of the statistical oval at 1430 UT.

view straddle noon in magnetic local time (MLT) and hence are in an optimum position to observe convection and backscatter features associated with the cusp region.

We present observations of the northern and southern cusp regions by these two radars following a southward turning of the interplanetary magnetic field (IMF) detected by the IMP-8 solar wind monitor at approximately 1350 UT on 17 April 1996. (The interested reader is directed to the study of Milan *et al.* (1999c) which has previously investigated the Northern Hemisphere dynamics observed during this interval.) At this time, the spacecraft was located near $X_{GSE} \approx 30 R_E$, $Y_{GSE} \approx -15 R_E$, and $Z_{GSE} \approx 22 R_E$, that is approximately $15 R_E$ upstream of the subsolar bow shock. The solar wind speed of approximately $450\,km\,s^{-1}$ suggests that a solar wind propagation delay of 10 to 15 min should be expected between the IMF being observed at IMP-8 and it impinging on the subsolar magnetopause, and this is found to be consistent with the ionospheric observations (see below). Figure 2e presents the IMF observations from this period in GSM coordinates, time shifted by 10 min for comparison with the radar data shown in the upper panels of the figure. In this shifted time-frame negative turnings of all three components of the magnetic field are seen just prior to 1400 UT. Following this turning the IMF remains moderately constant for upwards of 1.5 hours. Most importantly, the north-south component B_z is negative, approximately -4 nT, though with a brief excursion to 0 nT near 1435 UT. B_y varies between -1 and -4 nT

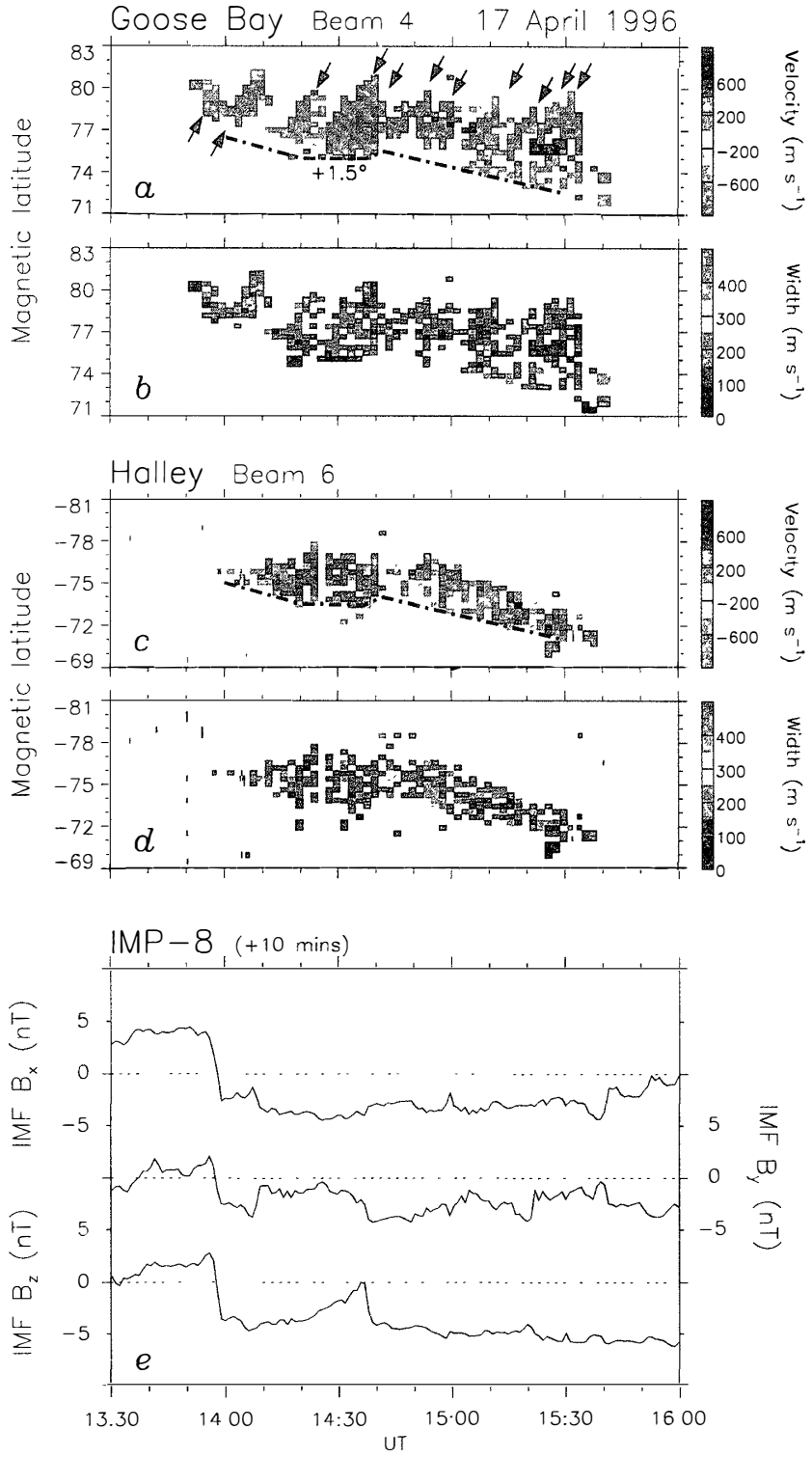

Fig. 2. (a) Line-of-sight velocity, magnetic latitude, time plot of the observations from beam 4 of the Goose Bay radar for 1330 to 1600 UT, 17 April 1996. (b) Similar to (a) though the spectral width measurements. (c) and (d) Similar to (a) and (b), though for beam 6 of the Halley radar. Panels (a) and (c) have the same model OCB motion superimposed (dot-dashed line), though that in panel (a) is shifted poleward by 1.5° in latitude. (e) IMP-8 measurements of the B_x, B_y and B_z components of the IMF, time-shifted by 10 min to account for the solar wind propagation delay.

during this interval, with B_x taking values near -3 nT.

The radar observations, line-of-sight Doppler velocity and spectral width, from beam 4 of Goose Bay and beam 6 of Halley are shown in the upper panels of Fig. 2. Negative and positive Doppler velocities represent flow away from and towards the radar, that is polewards and equatorwards in these meridionally-pointing beams, respectively. Prior to approximately 1350 UT no backscatter is observed. Radar echoes are then first observed by the Goose Bay radar, followed a few minutes later by Halley. The appearance of backscatter seems, then, to be closely associated with the southward turning of the IMF observed by IMP-8. Backscatter continues to be observed by both radars until about 1540 UT, though there is no clear precursor in the IMF for the loss of radar echoes at this time. The equatorward edge of the backscatter, especially that observed by the Halley radar, is well-defined and has been approximately delineated by a dot-dashed line superimposed on Fig. 2c. This line indicates that between 1400 and 1420 UT the equatorward edge of the backscatter progresses equatorward in geomagnetic latitude from 75°S to 73.5°S. The equatorward edge then remains at a constant latitude until 1440 UT, at which time there is a small jump poleward to 74°S. Thereafter the boundary moves equatorward to 71°S by 1530 UT. Overall, then, this boundary moves equatorwards by 4° of latitude in 90 min. The equatorward edge of the Goose Bay scatter is not as well defined, but follows a very similar trend to that described above, except that on average it is found 1.5° further poleward than in the conjugate hemisphere: the dot-dashed line in Fig. 2a displays the same latitudinal variation as that in Fig. 2c only displaced by 1.5° in latitude. The pause in the equatorward progression of this boundary, observed in both hemispheres between 1420 and 1440 UT, appears to be associated with the interval during which the B_z component of the IMF becomes less negative and near-zero; the resumption of equatorward motion accompanies the negative step in B_z. Moreover, there appears to be a brief (~4 min) but significant reduction in the line-of-sight velocity observed by the Halley radar at the time of the poleward step, approximately 1442 UT. These responses to changes in the IMF appear to confirm the approximate solar wind delay suggested above.

Poleward of this equatorward boundary, the appearance of the two regions of backscatter have marked differences. The Goose Bay region of scatter is on average 4° to 5° in latitudinal width, whereas the Halley backscatter is narrower at only 2° to 3° in width. Furthermore, the Goose Bay backscatter takes the form of many poleward-moving features, indicated by arrows in Fig. 2a, which as mentioned in the introduction have been identified as the radar counterpart of poleward-moving auroral forms (PMAFs) associated with flux transfer events (FTEs), that is bursts of magnetopause reconnection. The Halley observations, although conjugate to the Goose Bay observations, do not show these characteristic radar PMAFs. Careful inspection of the Goose Bay observations allows at least 11 PMAFs to be identified during the 100 min or so in which backscatter is present. This gives an average repetition rate of one every 9 min, close to the typical recurrence rate of FTEs (see McWilliams *et al.* (2000) and references therein).

The line-of-sight velocity observed by both radars in the meridional beams presented in Fig. 2 is negative, or in other words the north-south component of the plasma drift near local noon is directed polewards. Both radars observe an average poleward

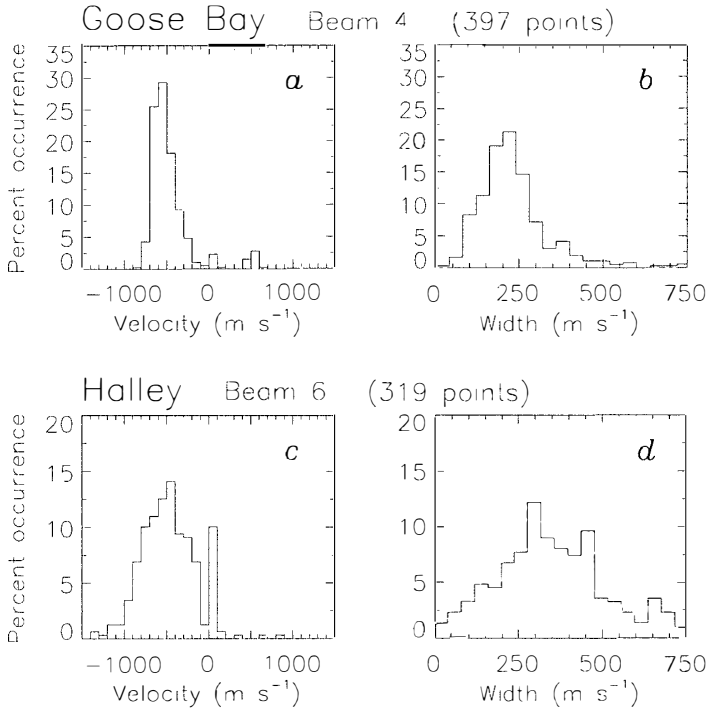

Fig. 3. Distributions of line-of-sight velocity and spectral width measurements from beams 4 and 6 of the Goose Bay and Halley radars, respectively.

component of the plasma drift of close to 600 m s^{-1}, though the velocity field observed by Goose Bay appears smoother than that observed by Halley which displays considerable variability in both time and latitude. This is shown more quantitatively in Fig. 3, in which panels a and c represent occurrence distributions of the line-of-sight velocities observed in Fig. 2: the distribution of Halley is markedly broader than that of Goose Bay. The preponderance of line-of-sight velocities near zero in Fig. 3c is a consequence of ground clutter. The backscatter spectra observed by both radars are broad, with spectral widths in general greater than 150 m s^{-1}. Figure 3b and d present occurrence distributions of the spectral widths observed in Fig. 2. Baker *et al.* (1995) identified high spectral width backscatter, in which the spectral width distribution was similar to those found in Fig. 3, as characteristic of the cusp, whereas low spectral width echoes were associated with the low latitude boundary layer (LLBL). Indeed, a steep latitudinal gradient in spectral width is sometimes observed in dayside HF radar backscatter measurements, interpreted as the boundary between these two magnetospheric regions, but just as often solely the cusp region is apparent (Milan *et al.,* 1999b; Moen *et al.,* 2000), as in the observations presented in Fig. 2. We note that equatorward of the main region of backscatter in Fig. 2c small regions of low spectral width echoes are observed. This is seen more convincingly in more easterly beams in the Halley radar field-of-view, illustrated in Fig. 4 which presents backscatter power, line-of-sight velocity, and spectral width measurements from beam 10. Superimposed on each panel is the same dot-dashed line found in Fig. 2c. Here, scatter is observed at lower latitudes than this boundary, especially between 1400 and 1440 UT, and this scatter tends to be of significantly lower spectral width than the higher latitude "cusp" scatter (see Fig. 4c). Moreover, these lower latitude, low spectral width "LLBL" echoes are also of significantly lower return power, some 10 dB down on the cusp scatter (Fig. 4a), indicating that the ionospheric irregularities in this region have a relatively low backscatter

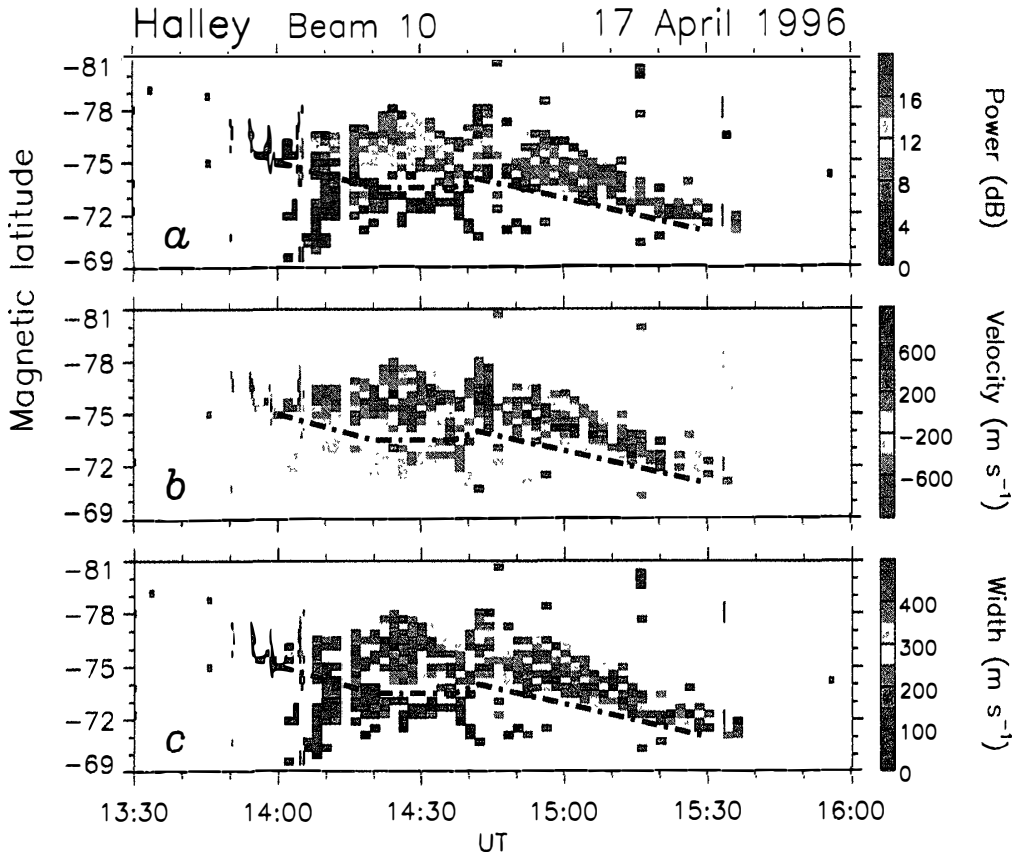

Fig. 4. Similar to Fig. 2, though the backscatter power, line-of-sight velocity and spectral width measurements from beam 10 of the Halley radar. The same model OCB motion as that presented in Fig. 2c is superimposed on each panel.

cross-section. That is, a steep latitudinal gradient in the backscatter power tends to be co-located with the steep gradient in the spectral width. For this reason the low-cross-section LLBL region is not always observed in conjunction with the high-cross-section cusp region, but the equatorward edge of the cusp region is indeed a "hard target" (Milan *et al.,* 1998) and can act as a reasonable proxy for the OCB.

We return to the radar observations to investigate the nature of the FTE signatures seen by Goose Bay in more detail, and to contrast these with the Halley observations. Figure 5 shows a sequence of radar scans from both radars from the interval 1448 to 1500 UT. Line-of-sight velocity data are presented in a magnetic latitude and magnetic local time coordinate system, curved dotted lines representing 70° and 80° latitude and straight dotted lines MLT meridians with 12 MLT towards to top of each panel. The dashed lines indicate the extremes of the radar fields-of-view. Lastly, two solid curved lines represent the poleward and equatorward edges of the statistical auroral oval. Panels a–d show radar scans from the Goose Bay radar and panels e–h show simultaneous scans from the Halley radar. Within each sequence the panels are separated by 2 or 4 min, that is one or two radar scans. Panels i and j show enlargements of panels c and g (1456 UT), superimposed on which are 2-dimensional velocity vectors determined by a beam-swinging technique (*e.g.* Ruohoniemi *et al.,* 1989; Milan *et al.,* 2000). The dot-dashed lines in these panels show the locations of beams 4 and 6 of the Goose Bay

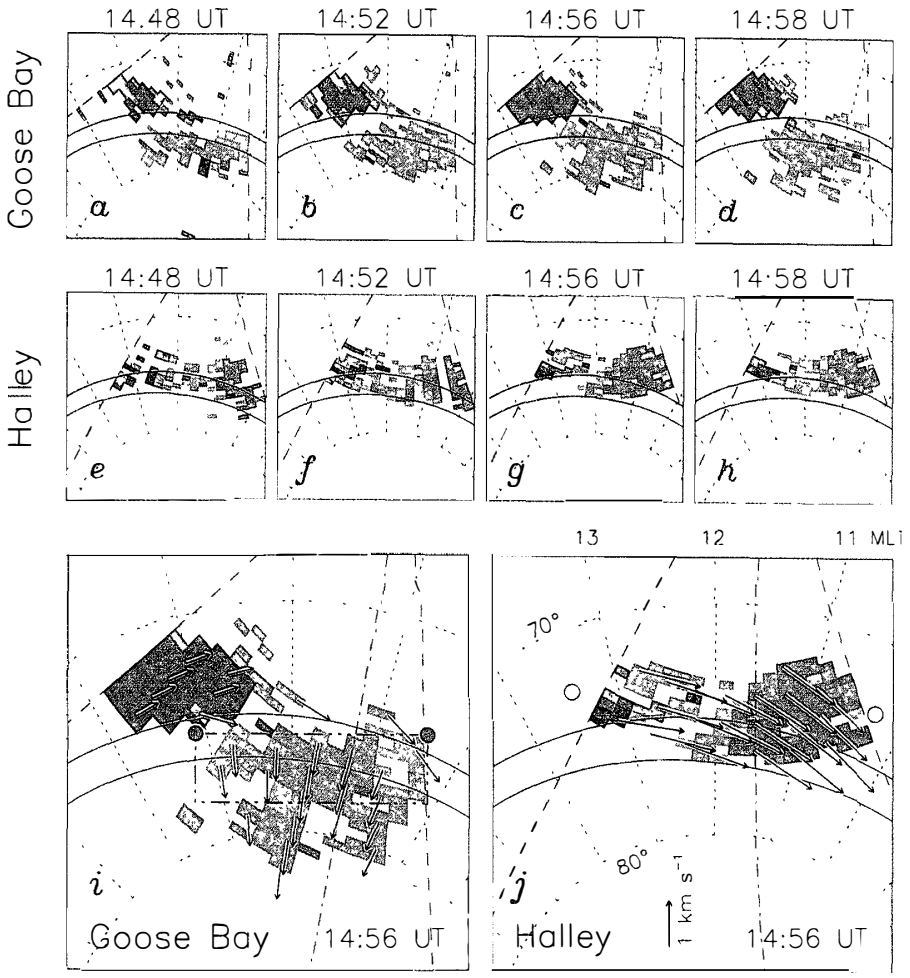

Fig. 5. (a)–(d) Four Goose Bay radar scans from the interval 1448 to 1458 UT, displayed in magnetic latitude, magnetic local time coordinates. (e)–(f) Similar to (a)–(d), though for the Halley radar. (i) A reproduction of panel (c), enlarged to show velocity vectors determined from a beam-swinging technique. Also shown are the Northern Hemisphere footprints of the field lines modeled in Fig. 5 (filled circles), the location of beam 4 of the radar (dot-dashed line) and an area equivalent to the estimated flux opened by an individual FTE, see text for details (dot-dot-dashed box). (j) Similar to panel (i) though for the Halley radar. Open circles represent the Southern Hemisphere footprints of the field lines displayed in Fig. 6.

and Halley radars, respectively, from which the observations of Fig. 2 were taken.

First we describe the Goose Bay observations. Two regions of backscatter are clearly discernable, in more easterly beams a region of positive line-of-sight velocities and in more westerly beams a region of negative velocities. As will be discussed below we interpret the positive-velocity region (plasma drift toward the radar) as return flow. The negative velocity backscatter region, approximately 2.5 to 3 hours of MLT wide, represents flow into the polar cap and it is here that the FTE signatures are seen, and hence it is on this region that we concentrate. The beam-swinging analysis presented in Fig. 5i suggests that in this region the plasma flow is directed more or less poleward, though with a small component towards the dusk sector, with a velocity between 600 and 800 m s^{-1}. One FTE signature is observed in the sequence of Goose Bay scans

shown in Fig. 5a–d. At 1448 UT the region of negative velocities is relatively narrow (~3°) in latitudinal extent. In the next two panels, this region of backscatter extends both equatorward and poleward, to reach its maximum latitudinal extent of 5° to 6° by 1456 UT. In the following panel, at 1458 UT, it is clear that the poleward portion of this region of backscatter is beginning to fade (indeed, there is some evidence that it has broken away from the more equatorward portion) and the equatorward boundary of this region has begun to retreat poleward once more. In the subsequent scan (not shown) the backscatter region returns to its original configuration. Note that throughout this sequence the plasma drift velocities measured by the radar do not vary significantly.

Turning to the simultaneous Halley observations in Fig. 5e–h, the main finding is that there is no clear FTE signature at this time (or throughout the rest of the interval) similar to that observed by the Goose Bay radar. Moreover, although the line-of-sight velocities observed in easterly beams are positive and in westerly beams are negative, as observed by Goose Bay, there is a relatively smooth variation between these extremes in the central beams. This pattern of line-of-sight velocities is consistent with flow which has a significant azimuthal component. The beam-swinging analysis of these velocities (Fig. 5j) indicates that the plasma drift has a speed of some 1400 m s^{-1} and is directed at an azimuth of 65° west or dawnwards of magnetic south. This gives poleward and westward components of the flow near 600 m s^{-1} (consistent with previous estimates) and 1250 m s^{-1}, respectively.

3. Discussion

In this discussion we employ the radar observations to determine the electrodynamics of the dayside coupling process. We start by estimating the reconnection voltage. As we have already discussed, the equatorward boundary of the backscatter observed by the two radars in Fig. 2 can be interpreted as a proxy for the OCB. The equatorward motion of the OCB during the interval of interest is consistent with the accumulation of open flux in the polar cap by magnetopause reconnection, expected when IMF $B_z < 0$ nT. This assertion is strengthened by the pause in the equatorward motion of the OCB when $B_z \approx 0$ nT around 1430 UT. Put another way, the equatorward motion of the OCB is related to the well-known equatorward motion of the auroral oval during substorm growth phase. The rate of change of area of the polar cap is related to the day- and nightside reconnection rates through the following statement of Faraday's Law (*e.g.* Lockwood and Cowley, 1992; Lewis *et al.,* 1998):

$$B \frac{dA}{dt} = \Phi_d - \Phi_n .$$

Here A is the area of the polar cap, B is the ionospheric magnetic field intensity, and so BA is the amount of open flux contained within the polar cap. Φ_d and Φ_n are the day- and nightside reconnection voltages, respectively, which are the integrals of the reconnection electric field along the day- and nightside reconnection lines (sometimes called merging gaps) either along the X-lines themselves or along their projections in the ionosphere. If the dayside reconnection electric field in the ionosphere E_{di} or at the

magnetopause E_{dm} is assumed to be constant along the reconnection line then $\Phi_d = E_{dl} L_{dl} = E_{dm} L_{dm}$ where L_{dl} and L_{dm} are the lengths of the X-line in the ionosphere and at the magnetopause, respectively. A similar expression exists for Φ_n. Finally, E_{dl} can be related to plasma drifts that are excited in the ionosphere by reconnection through the relationship $v' = E_{dl} \times B/B^2$ where v' is the boundary-normal drift velocity relative to the OCB.

If the observed equatorward progression of the OCB occurs equally at all local times, that is we assume that the polar cap remains approximately circular, then the area of the polar cap is initially 8.8×10^6 km^2 (OCB latitude 75°), expanding to 14.0×10^6 km^2 (latitude 71°) after 90 min. This represents an average rate of change of area of 9.6×10^2 km^2 s^{-1} or, assuming that $B = 5 \times 10^{-5}$ T, the rate of increase of flux in the polar cap is 4.8×10^4 Wb s^{-1}. If we assume that little or no reconnection occurs in the magnetotail during this interval ($\Phi_n \approx 0$), this is directly equivalent to the dayside reconnection voltage, that is 48 kV. From the plasma drift measurements made by the radars we can estimate the average reconnection electric field. The poleward plasma drift speed is approximately 600 m s^{-1} and the average equatorward speed of the OCB is 80 m s^{-1} (4° in 90 min), hence the mean plasma drift speed across the OCB is 680 m s^{-1}. We must assume that this is the boundary-normal speed as we are interested in the electric field along the boundary, but this appears to be a reasonable assumption as our measurements are made along meridionally-pointing radar beams. As $v' = E_{dl}/B$, the electric field in the frame of reference of the OCB is then 34 mV m^{-1}. It is then straight-forward to see that the ionospheric footprint of the reconnection line must be approximately 1400 km in length, equivalent to a little less than 3 hours of MLT at cusp latitudes, to supply the 48 kV needed to account for the estimated rate of expansion of the polar cap. This is consistent with the Goose Bay radar observations, in which the azimuthal extent of the region of backscatter corresponding to flow into the polar cap was seen to be some 2.5 to 3 hours of MLT (see Fig. 5i). Hence we can be confident that we are observing the totality of the merging gap or convection throat with this radar.

In addition we can estimate the reconnection electric field at the magnetopause based on the upstream IMF conditions, using the technique described by Lewis *et al.* (1998). Employing this method we acquire a mean value of the electric field during the interval of interest of $E_{dm} = 0.4$ mV m^{-1}, which requires that the length of the reconnection line at the magnetopause be of order 18 R_E for the reconnection voltage to total 48 kV. We can employ the Tsyganenko (1989) T89 magnetic field model to test if this is consistent with the radar observations. In Fig. 5i two filled circles have been superimposed to represent our estimate of the width of the ionospheric projection of the reconnection X-line. These are then employed as the footprints of magnetic field lines which we trace out to the magnetopause and into the Southern Hemisphere. The mapping of these two field lines is presented as solid curves in the X-Z, X-Y, and Y-Z planes (in GSM coordinates), in Fig. 6. Dashed lines show the approximate locations of the magnetopause and bow-shock. From this mapping we determine a reconnection X-line length at the magnetopause of ~17 R_E, remarkably close to the estimate of 18 R_E gained from our previous calculations. The Southern Hemisphere footprints of these field lines are represented by open circles in Fig. 5j. A tolerably good correspon-

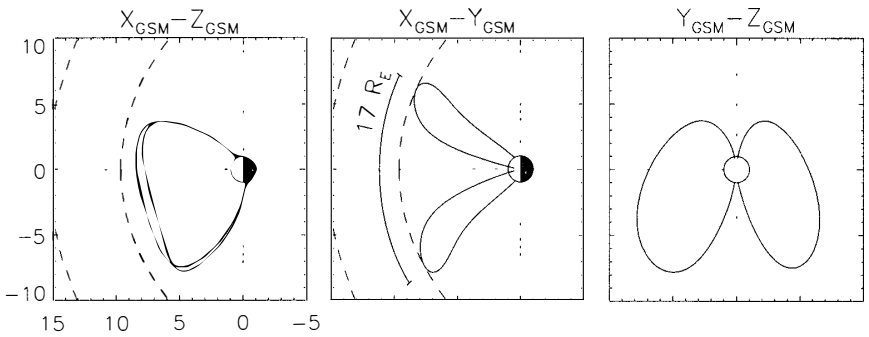

Fig. 6. Tsyganenko T89 magnetic field line mappings for field lines close to the ends of the ionospheric projection of the reconnection X-line determined from the Goose Bay radar observations (see Fig. 6i and j for the footprints of these field lines in the Northern and Southern Hemispheres, respectively). The mappings are displayed in GSM coordinates in the X-Z, X-Y and Y-Z planes. Model locations of the magnetopause and bowshock are shown in the X-Z and X-Y planes.

dence to the latitude of the equatorward boundary of the backscatter region is found. Importantly, this also suggests that the OCB is located at lower latitude in this hemisphere than in the Northern Hemisphere, corresponding to the latitudinal shift first identified in Fig. 2. A further finding is that in the Southern Hemisphere the reconnection X-line appears to map to a footprint extending right across the radar field-of-view, which is maybe 1700 km in length. If this is the case, the average reconnection electric field in the ionosphere is expected to be only 80% of that in the Northern Hemisphere. Indeed, such a disparity in the poleward component of the plasma drifts was suggested by the beam-swinging analyses presented in Fig. 5i and j.

We now turn our discussion to the Goose Bay signatures of FTEs. The sequence of cartoons in Fig. 7 present our interpretation of these observations. Initially, a region of backscatter is observed whose equatorward boundary, closely associated with the OCB, is located at a latitude Λ (Fig. 7a). The poleward component of the plasma drift or convection speed is v_{plasma} (observationally approximately 600 to 800 m s^{-1}). We identify this with a region of recently opened flux, the flux opened by the most recent burst of reconnection. At the outset of our sequence of images no reconnection is occurring and so the OCB must be moving with the plasma, $v_{OCB}=v_{plasma}$, and the OCB is said to be "adiaroic", meaning "no flow across" (Siscoe and Huang, 1985). When a subsequent burst of reconnection occurs new flux is appended to the polar cap (Fig. 7b). The reconnection electric field is non-zero, so the OCB moves relative to the background plasma, $v_{OCB}\neq v_{plasma}$, where the boundary-normal plasma drift is $v'=v_{plasma}-v_{OCB}$. If v' is sufficiently large then $v_{OCB}<0$ and the OCB migrates equatorwards. Observationally, the equatorward speed of the OCB during bursts of reconnection is close to 600 m s^{-1}, though this is a difficult measurement to make with the sampling resolution available from the radar scans. This speed can be deduced from Fig. 5a–c in which the boundary is observed to migrate equatorwards by some 2.5° of latitude in 8 min. In this case, $v'\approx 1.2$ km s^{-1}, which gives a measure of the instantaneous reconnection electric field of ~64 mV m^{-1} (compared with an average of 34 mV m^{-1}). At this time the original region of recently opened flux continues to convect polewards at the convection speed and overall the region of backscatter appears to expand both polewards and

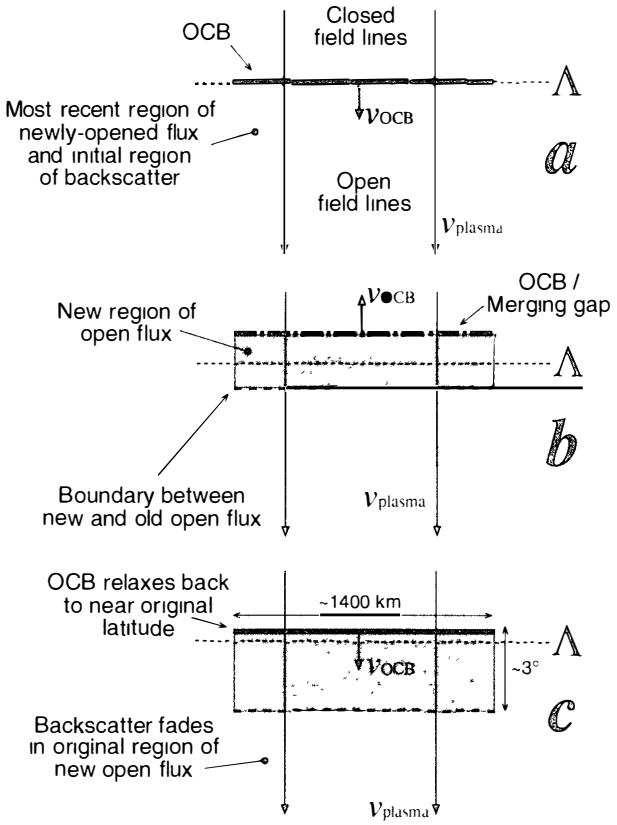

Fig. 7. A cartoon representing our interpretation of the radar observations of FTEs. See text for details.

equatorwards. Within a short period (a few minutes) reconnection wanes, the reconnection electric field becomes zero or near-zero, so once again $v_{OCB} = v_{plasma}$, and the equatorwards boundary of the backscatter region relaxes polewards at the convection velocity (Fig. 7c). The old region of open flux continues to be shunted into the polar cap, but its backscatter cross-section dwindles and eventually this region fades from view. We have now returned to the original situation, expect that perhaps the OCB is at a slightly lower latitude than before reconnection began, that is the polar cap has expanded slightly. In this way the OCB zig-zags equatorwards (when reconnection is on-going) and polewards (when reconnection has ceased) but with an overall equatorwards trend. Above we estimated the average reconnection electric field to be 34 $mV\,m^{-1}$, though now we can say that the instantaneous electric field was slightly less than twice this during bursts of reconnection and near zero at other times. This allows us to estimate that during the interval of study reconnection occurred approximately 50% of the time.

From the rate of expansion of the polar cap we can estimate the flux contained within each of the 11 individual FTEs as approximately 2.4×10^7 Wb, equivalent to an area of $4.7 \times 10^5\,km^2$. With the ionospheric projection of the reconnection X-line being 1400 km long, each FTE signature must be on average 335 km or 3° in latitudinal width. Our estimate of the area of flux appended by each FTE has been superimposed on Fig. 5i as a dot-dot-dashed rectangle. This spans the gap between the two field line footprints representing the extremes of the merging gap and extends 3° into the polar cap. This is found to correspond almost exactly to the lower half of the negative-velocity region of backscatter, which as we discussed above we interpret as the region of

new open flux. Hence, our estimate of the flux appended by each FTE, which we determined from the rate of expansion of the polar cap, matches very well the backscatter features we observe in the cusp region.

Our estimate of the area of flux in each FTE corresponds to, on average, 5% of the area of the pre-existing polar cap appended in each reconnection burst, close to the estimate of 3% made by Lockwood *et al.* (1990). Milan *et al.* (2000) provided another estimate of the FTE contribution to the area of the polar cap of 10%, though this was under more extreme loading conditions, IMF $B_z \approx -10$ nT, as opposed to $B_z \approx -4$ nT as during the present interval. As suggested by Milan *et al.,* it is possible that the size of FTEs is controlled by the upstream IMF conditions.

A schematic representing the backscatter regions observed by the two radars and their possible relationship to the dayside convection pattern is presented in Fig. 8. Arrowed curves show a convection pattern that is consistent with the IMF $B_y, B_z < 0$ nT, that is flow directed into the polar cap from the closed field line region, with an azimuthal component directed towards post-noon in the Northern Hemisphere and pre-noon in the Southern Hemisphere. In the Northern Hemisphere, stagnation occurs near the reversal in the post-noon convection cell, that is the convection electric field approaches 0 mV m^{-1}, closely co-located with the OCB. Milan *et al.* (1999a) demonstrated that ionospheric irregularities are not generated in regions of near-zero electric field and hence HF radar backscatter is not observed at this point, explaining the gap observed in the backscatter in the Goose Bay field-of-view. Elsewhere the convection flow is closely aligned along the beam pointing directions. As discussed above, we interpret the equatorward edge of the negative Doppler shift backscatter region as close to the OCB and/or merging gap. This interpretation places the positive Doppler shift backscatter in the return flow region, on closed field lines. This is then a problem for our understanding of the spectral width boundary, as the echoes in this region are no narrower than those on open field lines. In the Southern Hemisphere we again place

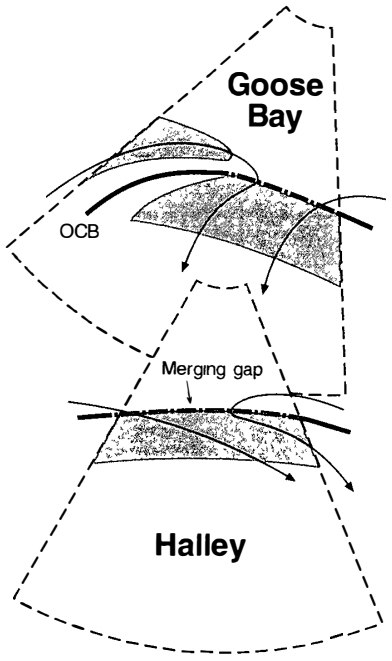

Fig. 8. A cartoon indicating our interpretation of the locations of the regions of backscatter within the Goose Bay and Halley radar fields-of-view with respect to the OCB and merging gaps. See text for details.

the OCB near the equatorward edge of the backscatter. In this hemisphere, however, the plasma drift has a much higher azimuthal component than at the conjugate location in the opposite hemisphere. There is, then, a significant asymmetry in the convection pattern in the conjugate hemispheres. That such an interhemispheric asymmetry is possible was suggested by the statistical seasonal asymmetry of the Northern Hemisphere convection response to IMF orientation found by Milan *et al.* (2001). This study demonstrated that the poleward component of plasma flow in the vicinity of the cusp was well-ordered by the B_z component of the IMF at all times of year, but the azimuthal component of the flow was most greatly modulated by B_y in summer months. It was suggested that this occurred as a consequence of biases introduced into the location of low latitude reconnection on the magnetopause by the tilt of the rotation axis of the Earth, that is the reconnection site would most often be located nearer the summer cusp than the winter cusp, and that this could produce an attendant increase in the influence of IMF B_y on the convective flow in the summer hemisphere. The present observations are made nearer equinox than solstice, but as the IMF B_x component is negative, the reconnection site is expected to occur closest to the Southern Hemisphere cusp. Here, then, the influence of IMF B_y on the convection pattern is expected to be greatest, just as is observed.

Two further interhemispheric asymmetries exist in the radar observations, which we will discuss below. The first is the asymmetry in the spectral widths of the backscatter echoes from the cusp region, and the second is the lack of FTE signatures in the Southern Hemisphere.

As discussed previously, Baker *et al.* (1995) demonstrated that in general "cusp" region backscatter spectra are broad. Two suggestions have been put forward for why this may be so. Yeoman *et al.* (1997) suggested that this was a consequence of the high but inhomogeneous fluxes of soft magnetosheath ion precipitation associated with this region. Alternatively, Andre *et al.* (1999) have postulated that high frequency (Pc1) wave activity associated with the cusp results in highly variable electric fields which broaden the spectra. We note, however, that the spectral width boundary observed between "LLBL" and "cusp" scatter is not peculiar to dayside HF radar observations, but is also clearly evident on the nightside (*e.g.* Lester *et al.,* 2001), and so whatever mechanism is responsible for broadening return echoes on open field lines is not specific to the "cusp" region alone. We wish to draw attention to one further aspect of the spectral width observations. Comparing Fig. 2b and d or Fig. 3b and d it is clear that although the spectra observed by both radars are broad, those observed by the Halley radar are broader than those observed by the Goose Bay radar. While both the Goose Bay and Halley distributions are dominated by the "cusp" spectral width signature identified by Baker *et al.* (1995) as opposed to narrow spectra characteristic of the "LLBL", the two distributions have modes near 200 and 300 m s^{-1}, respectively, and the latter is much broader than the former. It is also the Halley backscatter which has the more variable drift speeds (*cf.* Fig. 3a and c), as noted above. The reason for this interhemispheric asymmetry in the spectral width observations is not known. We do not presently know if this variation in spectral width is in some way dependent on the upstream solar wind or IMF conditions, or on the local ionospheric conditions, and hence provides additional information regarding the state of the cusp.

Finally, while FTE signatures are clearly apparent in the Northern Hemisphere, no discernable signature is observed in the Southern Hemisphere. One possibility to account for this is that the cusp is not located within the Halley radar field-of-view. If the B_y component of the IMF was large then the footprint of the reconnection site might be located in the early pre-noon sector in one hemisphere and in the late post-noon sector in the other. In such a case, signatures may be observed in one radar field-of-view but not the other. However, in the present case, the radar fields-of-view are located at noon, IMF B_y is relatively small, and field-line mapping confirms the expected conjugacy. This suggests that: (i) the mapping of the footprint of the reconnection site is not as we naively expect it; (ii) HF radars are not always sensitive to the ionospheric signatures of FTEs; or (iii) there can exist significant asymmetries in the ionospheric signatures of FTEs in conjugate hemispheres. Regarding the latter, the large azimuthal component of plasma flow in Southern Hemisphere could distort the FTE signature considerably, making it difficult to recognize in the radar observations. In relation to point (ii) we must consider what generation mechanisms might exist in the cusp region that will give rise to the ionospheric irregularities from which HF radars scatter. In the present interval, regions of backscatter in the Northern Hemisphere cusp region appear to delineate regions of newly opened flux. *F* region ionospheric irregularities are thought in general to arise through the action of ionospheric instability mechanisms (see review by Tsunoda, 1988), and two main candidates exist. The first is the current convective instability which could grow in the presence of the precipitation associated with the magnetopause reconnection processes. Once this source of precipitation is exhausted the backscatter region will fade, as observed. The second candidate is the gradient drift instability which can be excited if electron density gradients are formed perpendicular to the convection electric field. Hence, if reconnection processes in some way cause structuring of the ionospheric plasma in the cusp region then HF radar backscatter should be observed. As time progresses and these electron density gradients decay, the backscatter cross-section would be expected to diminish. Such structuring of the ionospheric plasma could be produced by particle precipitation, leading to enhancements in the electron density, or through heating of the plasma by high electric fields, that is fast flows, and the decrease in the electron density that this would entail. If electron density gradients are indeed responsible for the generation of the backscatter in which the FTE signature is observed, then factors such as the degree of solar illumination in each hemisphere could play a role in determining whether significant backscatter is generated or not.

4. Summary

During an interval of IMF $B_x, B_y, B_z < 0$ we have employed two SuperDARN radars observing the conjugate ionospheric cusp regions to estimate several quantities relating to the electrodynamics of dayside reconnection processes, and have shown our estimates to be internally consistent. We interpret the equatorward edge of high power, high spectral width backscatter as a proxy for the open/closed field line boundary (OCB). An equatorward motion of this boundary is seen to represent an accumulation of open flux in the polar cap, through low-latitude magnetopause reconnection, similar to the

interpretation of an equatorward motion of the nightside auroral zone by Lewis *et al.* (1998). From the rate of expansion of the polar cap we estimate the dayside reconnection voltage to be 48 kV. The poleward component of plasma drift in the two cusp regions is of order 600 to 800 m s^{-1}, giving a reconnection electric field in the ionosphere of ~35 mV m^{-1}, and a reconnection X-line footprint length of 1400 km, consistent with the azimuthal extent of the radar backscatter region observed in the Northern Hemisphere. A measurement of the reconnection electric field at the magnetopause from observations of the IMF, 0.4 mV m^{-1}, suggests that the magnetopause X-line must be 18 R_E in length. Field line mapping using the Tsyganenko T89 model shows that these estimates of the lengths of the magnetopause X-line and its ionospheric projection are consistent with each other. This mapping also suggests that the Southern Hemisphere OCB should occur at lower latitude than the Northern Hemisphere OCB, and indeed a 1.5° offset is observed by the radars.

The Northern Hemisphere radar observes 11 poleward-moving backscatter features, the signatures of flux transfer events (FTEs) or bursts of reconnection, with a repetition rate of some 9 min. On average, each FTE must produce a region of open flux which has an ionospheric cross-section of 4.7×10^5 km^2, approximately 5% of the area of the pre-existing open flux in the polar cap. With an azimuthal extent of 1400 km, this area of flux corresponds to a latitudinal extent of 3°, which is consistent with the radar observations. Throughout the sequence of FTEs little change is observed in the poleward component of the plasma drift, suggesting that the inductive smoothing effects discussed by Lockwood and Davies (1996) control the excitation of convection flows and that it is the OCB which moves in response to variations in the reconnection rate. Poleward and equatorward steps in the equatorward boundary of the radar backscatter, superimposed on the long-time scale equatorward trend of the OCB, appear to bear this out.

The Southern Hemisphere radar does not observe any significant signatures of bursty reconnection. Indeed, the convection flow patterns at the footprints of the reconnection X-line in the two hemispheres are found to be considerably different. That is, although the poleward component of the flow is similar in the two hemispheres (any difference being accounted for by differing lengths of the projection of the X-line), the azimuthal component of the plasma drift is near 0 km s^{-1} in the Northern Hemisphere and near 1.2 km s^{-1} in the Southern Hemisphere. It is suggested that because IMF $B_x < 0$ nT the magnetopause reconnection site is closest to the cusp footprint in the Southern Hemisphere.

The calculations described above are based on several assumptions: (1) the equatorward boundary of the radar backscatter is a good proxy for the OCB; (2) the equatorward motion of the OCB is the same at all local times; (3) very little reconnection occurs in the magnetotail during this interval (though the poleward step in the equatorward edge of the backscatter near 1440 UT suggests that some tail reconnection may occur at this time); (4) the poleward component of the drift velocity is the OCB-normal drift speed, or in other words that the ionospheric projection of the reconnection X-line lies along an L-shell. In addition, several interesting conclusions, but also perplexing questions, can be drawn from our observations:

(a) In the present interval, regions of backscatter in the cusp region delineate

regions of newly opened flux. We suggest that this backscatter is generated by: structuring of the plasma in the ionospheric footprint of the cusp region through (i) precipitation of magnetosheath particles producing electron density enhancements; or (ii) through ion-frictional heating and enhanced recombination rates; or (iii) that ionospheric irregularities are generated directly through field-aligned currents associated with precipitation, as suggested by Milan *et al.* (2000).

(b) Related to point (a), FTE signatures are apparent only in the Northern Hemisphere. This suggests either (i) a real asymmetry in the conjugate signatures of bursty reconnection, or (ii) an asymmetry in the HF radar signatures of bursty reconnection. In the latter case, a better understanding of the way in which radar backscatter is generated in the cusp region is needed.

(c) Previous studies have suggested that the equatorward boundary of the region of high spectral widths is a proxy for the OCB. In the present case this is co-located with a significant drop in the backscatter power, and for this reason, the low spectral width region equatorward of this is sometimes not seen. In cases such as this, it is the equatorward edge of the backscatter region itself that corresponds to the OCB. Sometimes a continuous region of backscatter is observed equatorward of FTE-related poleward-moving backscatter features, which has been interpreted as backscatter in the closed field line region, in other words the auroral oval (*e.g.* Milan *et al.,* 1999b, 2000). This again is not always observed, and the reason for this is unclear.

(d) The spectral widths observed in both hemispheres are consistent with the "cusp" designation of Baker *et al.* (1995), but spectral widths in the Southern Hemisphere are larger than in the Northern Hemisphere. These enhanced spectral widths also appear to be accompanied by a greater variability in the measured velocity field. Is this a real effect or a merely a consequence of the broad spectra giving more uncertain velocity estimates? Do the details of the spectral width occurrence distribution in either hemisphere give extra information regarding the reconnection signatures or the state of the cusp region ionosphere?

In conclusion, we have demonstrated that HF radars are excellent tools for studying dayside coupling processes. However, we have also identified several questions relating to the observation of the cusp region with HF radars. We hope that these questions will stimulate others to investigate some of these interesting phenomena.

Acknowledgments

SEM was supported by the Particle Physics and Astronomy Research Council (PPARC), U.K., grant no. PPA/G/O/1999/00181. The Goose Bay radar is operated under support of the U.S. National Science Foundation, grant no. ATM-9812078. The Halley radar was developed under funding from the Natural Environment Research Council (NERC), U.K., and the U.S. National Science Foundation, grant no. DPP-8602975. Operations are funded by the U.K. Natural Environment Research Council. The authors would like to thank the principle investigator, R. Lepping, for the use of key parameters from the IMP-8 MFI instrument.

The editor thanks Dr. J. Moen and another referee for their help in evaluating this paper.

References

Andre, R., Pinnock, M. and Rodger, A.S. (1999): On the SuperDARN autocorrelation function observed in the ionospheric cusp. Geophys. Res. Lett., **26**, 3353–3356.

Baker, K.B., Dudeney, J.R., Greenwald, R.A., Pinnock, M., Newell, P.T., Rodger, A.S., Mattin, N. and Meng, C.-I. (1995): HF radar signatures of the cusp and low-latitude boundary layer. J. Geophys. Res., **100**, 7671–7695.

Cowley, S.W.H. and Lockwood, M. (1992): Excitation and decay of solar wind-driven flows in the magnetosphere-ionosphere system. Ann. Geophys., **10**, 103–115.

Greenwald, R.A., Baker, K.B., Dudeney, J.R., Pinnock, M., Jones, T.B., Thomas, E.C., Villain, J.-P., Cerisier, J.-C., Senior, C., Hanuise, C., Hunsucker, R.D., Sofko, G., Koehler, J., Nielsen, E., Pellinen, R., Walker, A.D.M., Sato, N. and Yamagishi, H. (1995): DARN/SuperDARN: A global view of the dynamics of high-latitude convection. Space Sci. Rev., **71**, 761–796.

Lester, M., Milan, S.E., Besser, V. and Smith, R. (2001): A case study of HF radar spectra and 630.0 nm auroral emission. Ann. Geophys., **19**, 327–340.

Lewis, R.V., Freeman, M.P. and Reeves, G.D. (1998): The relationship of HF radar backscatter to the accumulation of open magnetic flux prior to substorm onset. J. Geophys. Res., **103**, 26613–26619.

Lockwood, M. and Cowley, S.W.H. (1992): Ionospheric convection and the substorm cycle. Proceedings of the International Conference on Substorms (ICS-1), 99–109 (ESA SP-335).

Lockwood, M. and Davies, C.J. (1996): On the longitudinal extent of magnetopause reconnection pulses. Ann. Geophys., **14**, 865–878.

Lockwood, M., Cowley, S.W.H. and Freeman, M.P. (1990): The excitation of plasma convection in the high-latitude ionosphere. J. Geophys. Res., **95**, 7961–7972.

Lockwood, M., Milan, S.E., Onsager, T., Perry, C.H., Scudder, J.A., Russell, C.T. and Brittnacher, M. (2001): Cusp ion steps, field-aligned currents and poleward-moving auroral forms. J. Geophys. Res. (in press).

Lu, G., Cowley, S.W.H., Milan, S.E., Sibeck, D.G., Greenwald, R.A. and Moretto, T. (2001): Solar wind effects of ionospheric convection: A review. J. Atmos. Solar-Terr. Phys. (in press).

McWilliams, K.A., Yeoman, T.K. and Provan, G. (2000): A statistical survey of dayside pulsed ionospheric flows as seen by the CUTLASS Finland HF radar. Ann. Geophys., **18**, 445–453.

Milan, S.E., Yeoman, T.K. and Lester, M. (1998): The dayside auroral zone as a hard target for coherent HF radars. Geophys. Res. Lett., **25**, 3717–3720.

Milan, S.E., Davies, J.A. and Lester, M. (1999a): Coherent HF radar backscatter characteristics associated with auroral forms identified by incoherent radar techniques: a comparison of CUTLASS and EISCAT observations. J. Geophys. Res., **104**, 22591–22604

Milan, S.E., Lester, M., Cowley, S.W.H., Moen, J., Sandholt, P.E. and Owen, C.J. (1999b): Meridian-scanning photometer, coherent HF radar and magnetometer observations of the cusp: a case study. Ann. Geophys., **17**, 159–172.

Milan, S.E., Lester, M., Greenwald, R.A. and Sofko, G. (1999c): The ionospheric signature of transient dayside reconnection and associated pulsed convection return flow. Ann. Geophys., **17**, 1166–1171.

Milan, S.E., Lester, M., Cowley, S.W.H. and Brittnacher, M. (2000): Convection and auroral response to a southward turning of the IMF: Polar UVI, CUTLASS and IMAGE signatures of transient flux transfer at the magnetopause. J. Geophys. Res., **105**, 15741–15756.

Milan, S.E., Baddeley, L.J., Lester, M. and Sato, N. (2001): A seasonal variation in the convection response to IMF orientation. Geophys. Res. Lett., **28**, 471–474.

Moen, J., Carlson, H.C., Milan, S.E., Shumilov, N., Lybekk, B., Sandholt, P.E. and Lester, M. (2000): On the correlation between dayside activity and coherent HF radar backscatter. Ann. Geophys., **19**, 1531–1549.

Neudegg, D.A., Yeoman, T.K., Cowley, S.W.H., Provan, G., Haerendel, G., Baumjohann, W., Auster, U., Fornacon, K.-H., Georgescu, E. and Owen, C.J. (1999): A flux transfer event observed at the magnetopause by the Equator-S spacecraft and in the ionosphere by the CUTLASS HF radar. Ann. Geophys., **17**, 707–711.

Neudegg, D.A., Cowley, S.W.H., Milan, S.E., Yeoman, T.K., Lester, M., Provan, G., Haerendel, G., Baumjohann, W., Nikutowski, B., Büchner, J., Auster, U., Fornacon, K.-H. and Georgescu, E. (2000): A survey of magnetopause FTEs and associated flow bursts in the polar ionosphere. Ann. Geophys., **18**, 416–435.

Pinnock, M., Rodger, A.S., Dudeney, J.R., Greenwald, R.A., Baker, K.B. and Ruohoniemi, J.M. (1991): An ionospheric signature of possible enhanced magnetic field merging on the dayside magnetopause. J. Atmos. Terr. Phys., **53**, 201–212.

Pinnock, M., Rodger, A.S., Dudeney, J.R., Baker, K.B., Newell, P.T., Greenwald, R.A. and Greenspan, M. E. (1993): Observations of an enhanced convection channel in the cusp ionosphere. J. Geophys. Res., **98**, 3767–3776.

Pinnock, M., Rodger, A.S., Dudeney, J.R., Rich, F. and Baker, K.B. (1995): High spatial and temporal resolution observations of the ionospheric cusps. Ann. Geophys., **13**, 919–925.

Provan, G. and Yeoman, T.K. (1999): Statistical observations of the MLT, latitude and size of pulsed ionospheric flows with the CUTLASS Finalnd radar. Ann. Geophys., **17**, 855–867.

Provan, G., Yeoman, T.K. and Milan, S.E. (1998): CUTLASS Finland radar observations of the ionospheric signatures of flux transfer events and the resulting plasma flows. Ann. Geophys., **16**, 1411–1422.

Provan, G., Yeoman, T.K. and Cowley, S.W.H. (1999): The influence of the IMF By component on the location of pulsed flows in the dayside ionosphere observed by an HF radar. Geophys. Res. Lett., **26**, 521–524.

Rodger, A.S. (2000): Ground-based imaging of magnetospheric boundaries. Adv. Space Res., **25**, 1461–1470.

Rodger, A.S. and Pinnock, M. (1997): The ionospheric response to flux transfer events: the first few minutes. Ann. Geophys., **15**, 685–691.

Rodger, A.S., Mende, S.B., Rosenberg, T.J. and Baker, K. B. (1995): Simultaneous optical and HF radar observations of the ionospheric cusp. Geophys. Res. Lett., **22**, 2045–2048.

Ruohoniemi, J.M., Greenwald, R.A., Baker, K.B., Villain, J.-P., Hanuise, C. and Kelly, J. (1989): Mapping high-latitude plasma convection with coherent HF radars. J. Geophys. Res., **94**, 13463–13477.

Siscoe, G.L. and Huang, T.S. (1985): Polar cap inflation and deflation. J. Geophys. Res., **90**, 543–547.

Tsunoda, R.T. (1988): High latitude F region irregularities: A review and synthesis. Rev. Geophys., **26**, 719–760.

Tsyganenko, N.A. (1989): A magnetospheric magnetic field model with a warped tail current sheet. Planet. Space Sci., **37**, 5–20.

Yeoman, T.K., Lester, M., Cowley, S.W.H., Milan, S.E., Moen, J. and Sandholt, P.E. (1997): Simultaneous observations of the cusp in optical, DMSP and HF radar data. Geophys. Res. Lett., **24**, 2251–2254.

(Received December 12, 2000; Revised manuscript accepted May 9, 2001)